Polymer Cable Characterization in Cable-Driven Parallel Robots

Sudarson Nanthacoumarane, Bozhao Wang, Afia Kouadri-Henni, Philippe Cardou, Stéphane Caro

Polymer Cable Characterization in Cable-Driven Parallel Robots

S. Nanthacoumarane[a], B. Wang[b], A. Kouadri-Henni[c], P. Cardou[d], S. Caro[e]

a. École Centrale de Nantes (ECN), sudarson.nanthacoumarane@eleves.ec-nantes.fr
b. Laboratoire des Sciences du Numérique de Nantes (LS2N), bozhao.wang@ls2n.fr
c. INSA Rennes, Laboratoire des Sciences du Numérique de Nantes (LS2N), Afia.Kouadri-Henni@ls2n.fr
d. Laboratoire de robotique, Département de génie mécanique, Université Laval, Philippe.Cardou@gmc.ulaval.ca
e. CNRS, Laboratoire des Sciences du Numérique de Nantes (LS2N), stephane.caro@ls2n.fr

Abstract :

The use of polymer cables in CDPRs allows the robot to extend to a large workspace and gives it a high effective payload to robot mass ratio. However, the complex viscoelastic nature of polymers makes it difficult to predict elongation of cables under load, which in turn affects the accuracy of the CDPR. Traditional methods of studying creep in cables require the use of expensive tensile testing machines. This study aims to inexpensively gather experimental data from static load tests conducted on polymer cables to study creep elongation over a prolonged period of time. These observations were then compared to known viscoelastic models in order to characterize the polymer cables.

L'utilisation de câbles en polymère dans les CDPR permet au robot de s'étendre à un grand espace de travail et lui confère un rapport charge utile effective/masse du robot élevé. Cependant, la nature viscoélastique complexe des polymères rend difficile la prédiction de l'allongement des câbles sous charge, ce qui affecte à son tour la précision du CDPR. Les méthodes traditionnelles d'étude du fluage des câbles nécessitent l'utilisation de machines d'essai de traction coûteuses. Cette étude vise à rassembler de manière peu coûteuse des données expérimentales provenant d'essais de charge statique réalisés sur des câbles en polymère afin d'étudier l'allongement par fluage sur une période prolongée. Ces observations sont ensuite comparées à des modèles viscoélastiques connus afin de caractériser les câbles en polymère.

Keywords : Parallel Robot, Polymer Cable, Creep, Viscoelasticity

Mots clefs : Robot parallèle, câble polymère, fluage, viscoélasticité

1 Introduction

Cable-driven parallel robots (CDPRs) are a sub-class of parallel robots that use cables to link the end-effector to actuators instead of rigid links [1]. The use of cables allows the robot to extend to a large workspace because cables are much lighter, longer, and more flexible than rigid links [2]. Moreover,

the use of cables gives CDPRs a high effective payload to robot mass ratio since cables can hold considerable loads in tension compared to rigid mechanical links. More specifically, polymer cables are preferred for use on CDPRs as they have several benefits over steel cables in terms of lightness, flexibility, cost, as well as safety [3].

Because of the large amount of passive joints and the cable flexibility, CDPRs may not have high accuracies. Besides, during the dynamic movements of CDPRs, the polymer cables withstand continuous loading and unloading process under varying forces and velocities. The complex viscoelastic properties of polymer cables make it difficult to predict their behaviours, including cable creep [4]. Creep is the time dependent elongation when the cables are subjected to long-term constant mechanical stress. Cable elongations due to creep is common in CDPR applications, and if they are not compensated, the errors on cable lengths will make it increasingly difficult to have accurate robot motions [5].

Static load test is the usual method used to obtain the creep curve [6]. Davies et al. [7] conducted cable tests in different scales, from single fiber to rope. For each load level, a long term loading/unloading phase was carried out. A video extensometer is used to record the elongation. In Ref. [5], the authors used a winch-cable-pulley system to easily handle high cable loads and long cable lengths. An optical tracking system is used to measure cable elongations with markers fixed on the cable. Choi et al. [4] conducted tensile experiments using different cable lengths with varying tensile rates to imitate the CDPR application. The tests are carried out with a tensile machine.

Plenty of polymer cable viscoelastic models have been proposed in previous studies. Most of them consist of two components : Maxwell model and Kelvin Voigt model, with Hookean spring and Newtonian damper joined in series and in parallel, respectively. Piao et al. [5] proposed a five-element model including the series combination of a spring and two Voigt models for a common polyethylene Dyneema polymer cable. Iurzhenko et al. [8] studied the properties of hybrid organic-inorganic polymer systems (HOIS) and proposed a Burgers four-element model. In Ref. [4], a nonlinear dynamic model for various tensile rates is proposed for Dyneema SK78 cables. Cable dynamic creep elongation is studied, including hardening effect.

This paper conducted various static loading and unloading tests on a Vectran® cable. Long time period cable elongations are recorded by a camera and a marker at the end of the cable. The test results are compared with known viscoelastic models [8] in order to find the one that best fits the experimental data. An analytical strain model for the cables was formed based on Burgers model, and this experimentally verified model can be used in CDPR cable control algorithms to improve the robot positioning accuracy. Section 2 describes the detailed experimental setup. Section 3 focuses on the important existing theoretical models for polymer models and introduces the algorithm used to obtain the test results. Finally, the results are analyzed and are compared with the known creep models.

2 Cable Characterizing Experiment

Vectran® is a high-performance multifilament yarn spun from liquid crystal polymer (LCP) manufactured solely by Kuraray Co., Ltd [3]. It has excellent mechanical properties, high abrasion resistance, and a very low rate of creep - all of which make it an ideal candidate for use in CDPRs. The mechanical properties of Vectran® are shown in Table 1 along with other industrial fibres for comparison, demonstrating that it has superior characteristics than some other conventionally used poly-

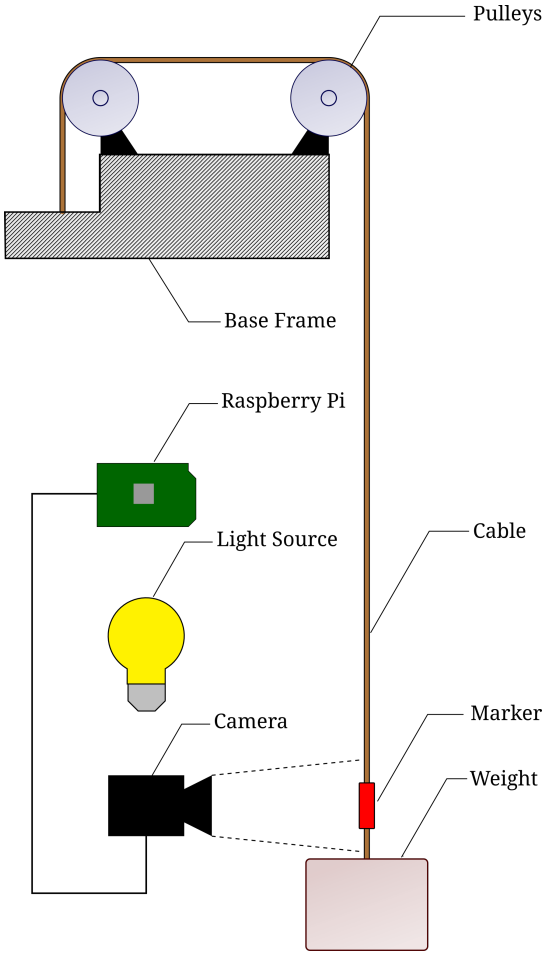

FIGURE 1 – Diagram of experimental setup

FIGURE 2 – Image capturing system

mers. The cable used in this experiment is an extended uncoated braid of Vectran® cable (VECT017LE), which has a diameter of 1.7mm and load rating of 250kg. The usual method of characterizing cables is by using a tensile testing machine [9]. However, it is not possible to test long lengths of cable this way, and the following section focuses on a cost effective way used to observe small changes in the elongation of a long cable.

2.1 Experimental Setup

In order to inexpensively obtain detailed information about Vectran® cables, a simple camera setup depicted in Fig. 1 was used to observe cable elongation over time. A two-megapixel camera was placed on a solid surface using a tripod, and focused on an adhesive marker which was placed near the end of the cable. This USB camera was controlled using a Raspberry Pi through a python script. A constant light source and heavy black curtains enclosing the experiment helped to maintain optimum lighting conditions to take photos. Weights could be loaded onto a lightweight aluminium holder, and this holder could easily be attached and detached from the end of cable using a carabiner. A detailed setup of this image capturing system can be seen in 2.

2.2 Experimental Procedure

The experiment was conducted by hanging a 9.7m length of cable from a height as depicted in Fig. 3 and exerting a constant force at the end of the cable in the form of a weighted mass. Since the length

Materials	Density (g/cm^3)	Tensile Strength (GPa)	Tensile Modulus (GPa)	Elongation at break (%)	Moisture regain (%)
Vectran®	1.40	3.4	70	4	<0.1
Aramid	1.44	3.0	65	4	4–6
UHMWPE	0.95	3.4	110	4	<0.1
Nylon	1.14	1.0	10	20	6–8
PET	1.38	1.1	14	15	<0.5

TABLE 1 – Fibre Mechanical Properties [3]

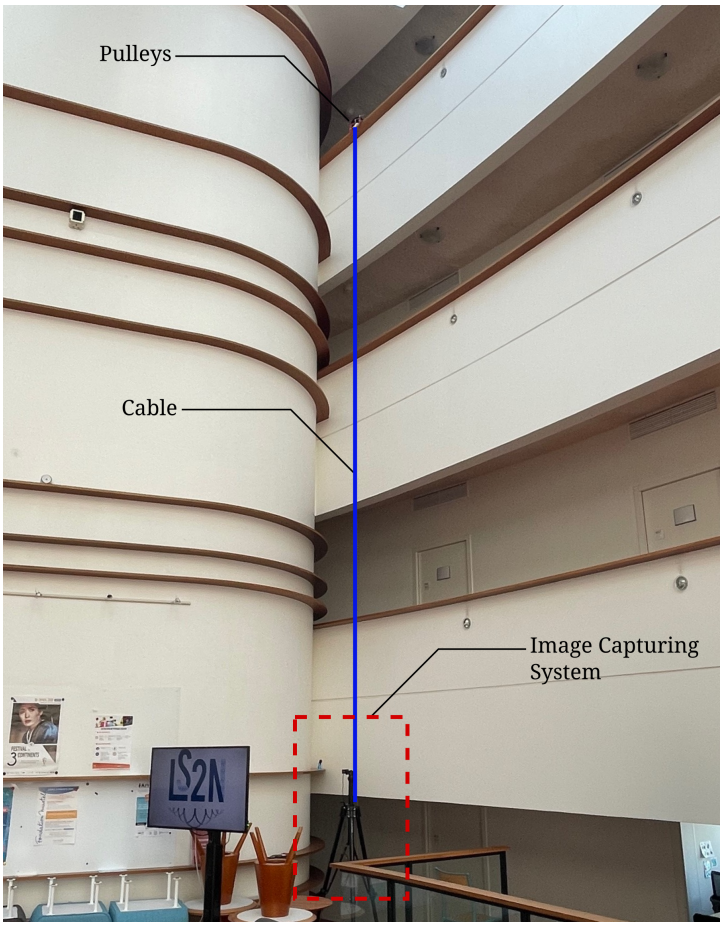

FIGURE 3 – Photo of full experimental setup

of the cable is quite long compared to its diameter, the cross section area of the cable is assumed to be constant, and therefore the stress on the cable for each weight can be considered to be constant. There are several stages of creep that a material goes through [10], and one cannot observe the later stages of creep if the experiment is conducted for a short period of time, especially without the influence of temperature to speed it up. Therefore, for each load, the cable was subject to 3 days of loading to observe elongation, and then a 2-day period of unloading to observe relaxation.

As the cable elongated under the influence of load, the adhesive marker on the cable would move across the photo frame of the fixed camera, and these photos would be saved onto an external me-

mory card on the Raspberry Pi. The photos of the cable marker could be taken at predetermined time intervals where the frequency of photo capture varied between 0.0033Hz and 1Hz. Photos were captured frequently during loading/unloading, but reduced in frequency as the experiment trials progressed and creep started to settle into the cable. In this manner, cable elongation could be measured efficiently and accurately by taking only 9000 photos of the cable over the course of the 24 day long experiment. The study was conducted by subjecting the same cable to various loads in order to observe creep under different loading conditions. The order of observation of these various loads are enumerated in Table 2.

Trial Characteristics	**Trial 1**	**Trial 2**	**Trial 3**	**Trial 4**
Mass (g)	1287.3	4349.9	8143.9	1287.3
Stress (MPa)	10.29	34.77	65.1	10.29
Loading Time (days)		3		
Unloading Time (days)		2		

TABLE 2 – Observation Details

2.3 Image Processing

The image algorithm took advantage of the fact that the marker on the cable was a contrasting colour to the colour of the cable. It is possible to determine the RGB colour value of each pixel and determine whether the pixel is part of the marker, the cable, or the background. By identifying pixels that belong to the marker, the centre of the marker can be found by taking an average of the horizontal and vertical positions of the marker pixels. Elongation in the cable can be measured by comparing the position of the marker centre in each frame to the initial position of the marker. The identification of the centre of the marker is depicted in Fig. 4. However, it is impractical to scan every pixel for each of the over 9000 images. Therefore, only the first image in each experiment was scanned from end to end, and then the range of the scan was reduced within 100 pixels of each previously identified position of the marker to reduce computing cost.

3 Creep Models and Parameter Estimation

3.1 Theoretical Creep Modelling

Creep is a slow, continuous deformation of a material under constant stress [10]. If left unchecked, creep can lead to mechanical failure well below the yield strength of the material. Several factors influence polymer cable creep behavior, including material mechanical properties, load values, length of cable, and temperature [5]. The cable diameter changes in a complicated way because of the cable internal configuration, however these changes are relatively small [4]. In this work, it is assumed that the experiments are conducted in room temperature and the temperature effect is neglected. The cable diameters is considered constant as well.

The most efficient way to predict the strain in polymers is to use the Burgers Viscoelastic Model [10] [11]. Hence we propose a standard Burgers element shown in Figure 5, itself consisting of a combination of a Maxwell element and a Kelvin-Voigt element, to explain the behaviour of polymer cables

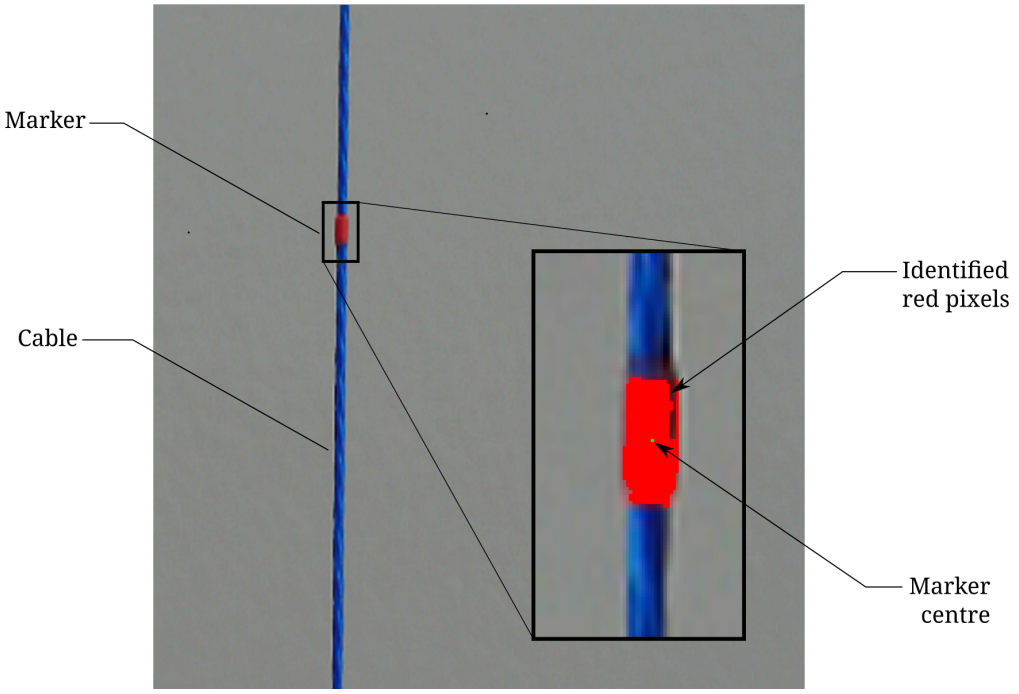

FIGURE 4 – Red pixels and centre of marker identified by algorithm

used in CDPRs. These models consist of two basic elements - a Hookean spring to describe linear strain, and a Newtonian damper or a dashpot to describe viscous strain. The spring of the Maxwell element represents the instantaneous elastic strain and its dashpot represents the non-reversible viscous flow. The Voigt element describes the delayed elasticity. We consider that the experiment starts at $t = 0$, loading takes place at $0 \leq t < t_1$, and unloading takes place at $t \geq t_1$, where t_1 is the point in time when load is removed from the cable.

Each element in the model contributes to a part of the strain exhibited by the polymer cable. ε_1 is the strain in the Maxwell spring, ε_2 is the strain in the Maxwell dashpot, and ε_3 is the strain in the Kelvin-Voigt element. The sum of these strains can be simply represented as :

$$\varepsilon = \varepsilon_1 + \varepsilon_2 + \varepsilon_3 \tag{1}$$

When subject to a constant stress σ_0, strains can be represented as a function of the material's rheological constants and applied stress :

$$\varepsilon_1 = \frac{\sigma_0}{E_1} \qquad \dot{\varepsilon}_2 = \frac{\sigma_0}{\eta_1} \qquad \dot{\varepsilon}_3 + \frac{E_2}{\eta_2}\varepsilon_3 = \frac{\sigma_0}{\eta_2} \tag{2}$$

The immediate linear increase in strain in $\overline{OA}$ seen in Fig. 5 is due to the Maxwell Spring, and the effect of the Maxwell dashpot and Voigt element can be seen across $\overline{AB}$. The stress-strain relations in Eq. (2) can be replaced in Eq. (1) to yield Eq. (3) for Loading Strain $\varepsilon_L(t)$ as suggested in Ref. [8] [12].

$$\varepsilon_L(t) = \sigma_0 \left[\frac{1}{E_1} + \frac{t}{\eta_1} + \frac{1}{E_2}(1 - e^{-E_2 t/\eta_2}) \right] \quad \forall \ \ t < t_1 \tag{3}$$

If stress σ_0 is removed at time t_1, the recovery behaviour of the Burgers model can be obtained using the superposition principle by considering at $t > t_1$ a constant stress $\sigma = -\sigma_0$ is added. This recovery

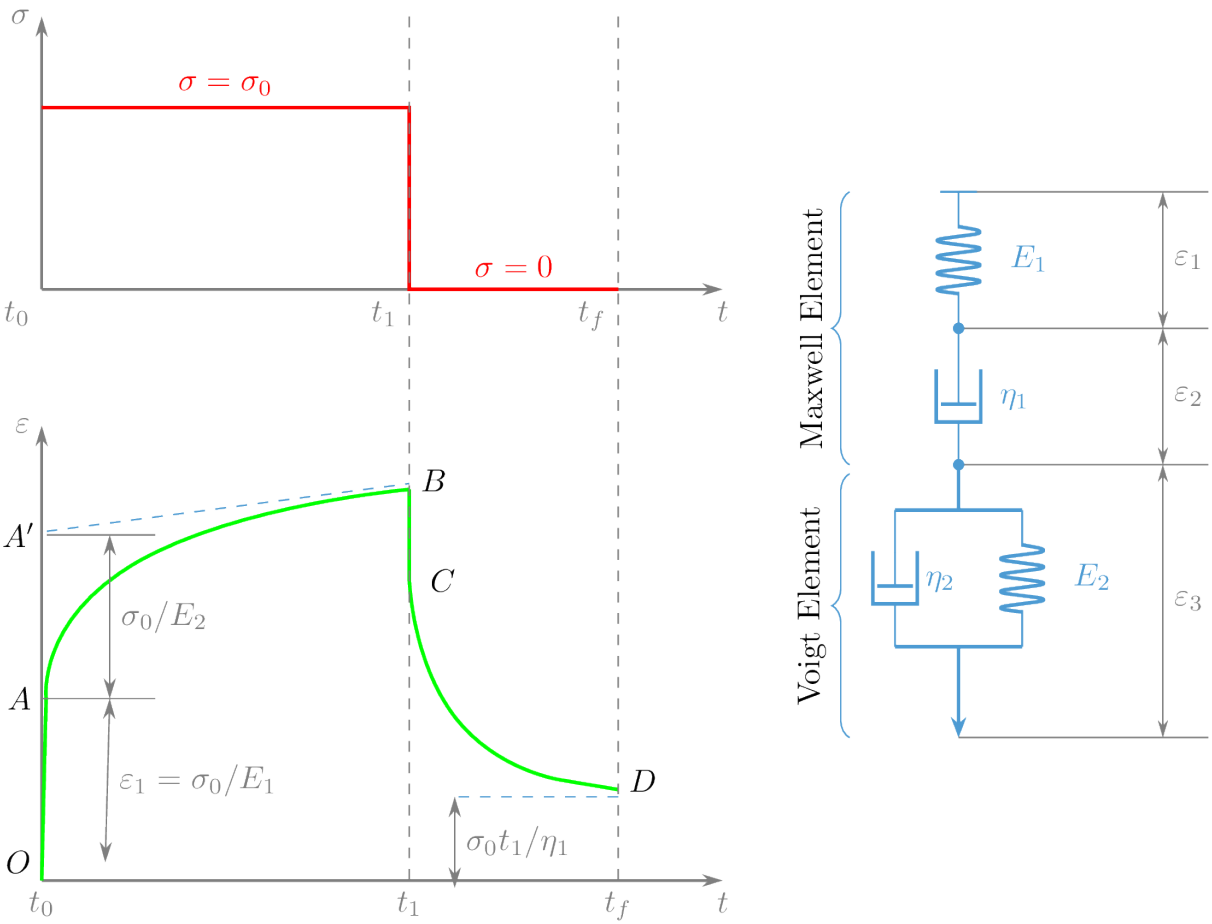

FIGURE 5 – Burgers Viscoelastic Model [10]

strain can be observed between $\overline{BD}$ in Fig. 5. According to the superposition principle, the recovery strain $\varepsilon_{UL}(t), t > t_1$ is the sum of these two independent actions as demonstrated in Ref. [10] :

$$\begin{aligned}\varepsilon_{UL}(t) = \sigma_0 \left[\frac{1}{E_1} + \frac{t}{\eta_1} + \frac{1}{E_2}(1 - e^{-E_2 t/\eta_2})\right] \\ - \sigma_0 \left[\frac{1}{E_1} + \frac{(t-t_1)}{\eta_1} + \frac{1}{E_2}(1 - e^{-E_2 (t-t_1)/\eta_2})\right]\end{aligned} \tag{4}$$

which can be then simplified to obtain unloading strain :

$$\varepsilon_{UL}(t) = \sigma_0 \left[\frac{t_1}{\eta_1} + \frac{1}{E_2}(e^{E_2 t_1/\eta_2} - 1)e^{-E_2 t/\eta_2}\right] \quad \forall \ t \geq t_1 \tag{5}$$

3.2 Non-linear data fitting

Based on the gathered data, it was noticed that the model parameters change as a function of mass and cable length, as noted in Ref. [5] and [13]. In order to characterize these parameter, the *lsqnonlin* function in © MATLAB was utilized. As the cable diameter is considered constant, the unknown decision variables to be determined are :

$$\mathbf{x} = \left[E_1\, E_2\, \eta_1\, \eta_2\right]^T \tag{6}$$

The cable strain is affected by each parameter. The elastic deformation at the beginning of each loading and unloading period is inversely proportional to E_1, the viscous deformation is inversely correlated to E_2, η_1 and η_2, and the residual plastic deformation at the end of each unloading period is inversely correlated to η_1.

The experimental measured cable deformation are first processed with a Butterworth digital filter, in order to reduce the high-frequency random noise on the deformation-time curve. For each loading and unloading period, an approximate 250s time interval is used to sample the measured data, shown in Fig. 7. This time interval allows the curve shape to be accurately shown and does not create redundant calculation points. The sampled points are the inputs of the problem. In such a way, approximately 2000 points are sampled during each loading/unloading period, and different sets of equations can be formulated with the difference between the calculated cable deformation d_c and the experimental measured deformation d_e :

$$f_i(\mathbf{x}) = d_c - d_e, \quad i = 1, \ldots, n \tag{7}$$

where $f(\mathbf{x})$ is the *lsqnonlin* objective function and n is the total number of sampled data in each period. It should be noted that the number of input values, namely, the number of equations, is much higher than the number of unknowns. Therefore, the nonlinear system of equations to be solved is overdetermined and can be solved with ©Matlab *lsqnonlin* function. The non-linear least square problem can be formulated as Eq. (8) :

$$\begin{aligned} \text{minimize} \quad & \sum_{i=1}^{n} f_i^2(\mathbf{x}) \\ \text{over} \quad & \mathbf{x} = \left[E_1\, E_2\, \eta_1\, \eta_2\right]^T \end{aligned} \tag{8}$$

The upper bounds, lower bounds and the initial values of the parameters need to be carefully selected. Knowing the effects of each parameter to the strain-time curve, the parameter values can be roughly chosen manually to fit the cable model as close as possible to the experiment measurements. Then the upper and lower bounds of those parameters are set accordingly at both sides of these rough values. During optimization, the initial parameter values are generated randomly within the upper and lower bounds.

If the optimized parameter values come very close to the bounds, the potential better optimization results maybe restricted. In those cases, the bounds are increased or decreased, in order to keep the optimized parameter values within the parameter bounds and with margins left. In such a way, the determination of the optimum parameter values for all of the four load periods is carried out. The evolutions of the parameter values with respect of the number of iterations of trial 1 are presented in Fig. 6. The comparison of the deformation versus time curve between the calculated cable deformation and the experiment measurements for the four load trials is shown in Fig. 7. Table 3 shows the optimized parameter values and the mean of every objective function absolute value during each period. According to the objective function values, the mean cable deformation error percentage of the initial cable length are calculated as :

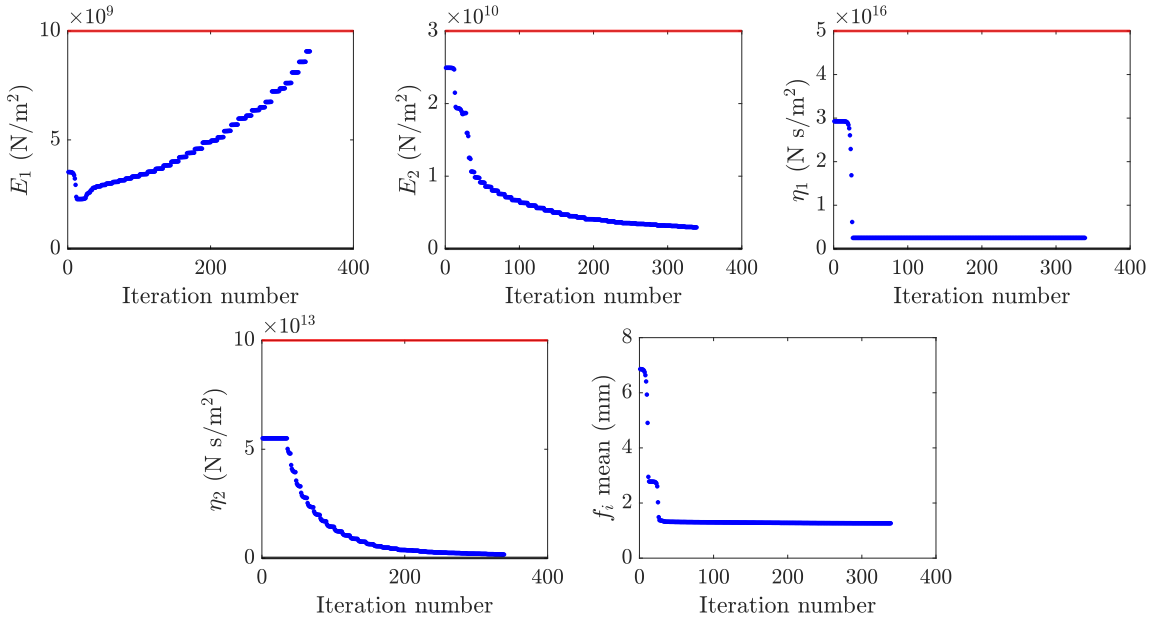

FIGURE 6 – Evolution of the decision parameters as a function of the iteration number, for trial 1

$$e_m = \frac{\sum_{i=1}^{n} |f_i|}{n l_0} \times 100 \tag{9}$$

Where l_0 is the initial cable length, e_m values for each load period are also summarized in Tab. 3. The errors between the proposed cable model and the experiment measurements are quite low compared with the cable length. For experiment trials 1, 2 and 4, the errors are lower than 0.02% of the cable length, for trial 3, the error percentage is less than 0.025%.

Parameters	**Trial 1**	**Trial 2**	**Trial 3**	**Trial 4**
E_1 (N/m^2)	9.07×10^9	5.60×10^9	7.78×10^9	3.66×10^9
E_2 (N/m^2)	2.95×10^9	2.23×10^{10}	2.28×10^{10}	8.14×10^9
η_1 (Ns/m^2)	2.50×10^{15}	6.91×10^{15}	8.97×10^{15}	7.43×10^{15}
η_2 (Ns/m^2)	1.67×10^{12}	2.10×10^{14}	2.39×10^{14}	4.38×10^{13}
f_i mean(mm)	1.26	1.60	2.42	1.12
e_m (%)	1.29×10^{-2}	1.64×10^{-2}	2.48×10^{-2}	1.15×10^{-2}

TABLE 3 – The summary of the optimized cable model parameters

Figure 8 shows the correlations and the variational trends between the objective function and the optimization decision variables of trial 1 by a scatter matrix, which was obtained with © MATLAB *plotmatrix* and *corrcoef* functions. The upper part of the matrix shows the scatter plots of the variables and objective function, and the lower part gives the corresponding correlation coefficients. The diagonal figures of the scatter matrix shows the probability density plot of each variable. The correlation coefficients change between -1 and 1. When two variables are more positively (negatively) dependent, the scatter plot will be closer to a positive (negative) linear shape, and the corre-

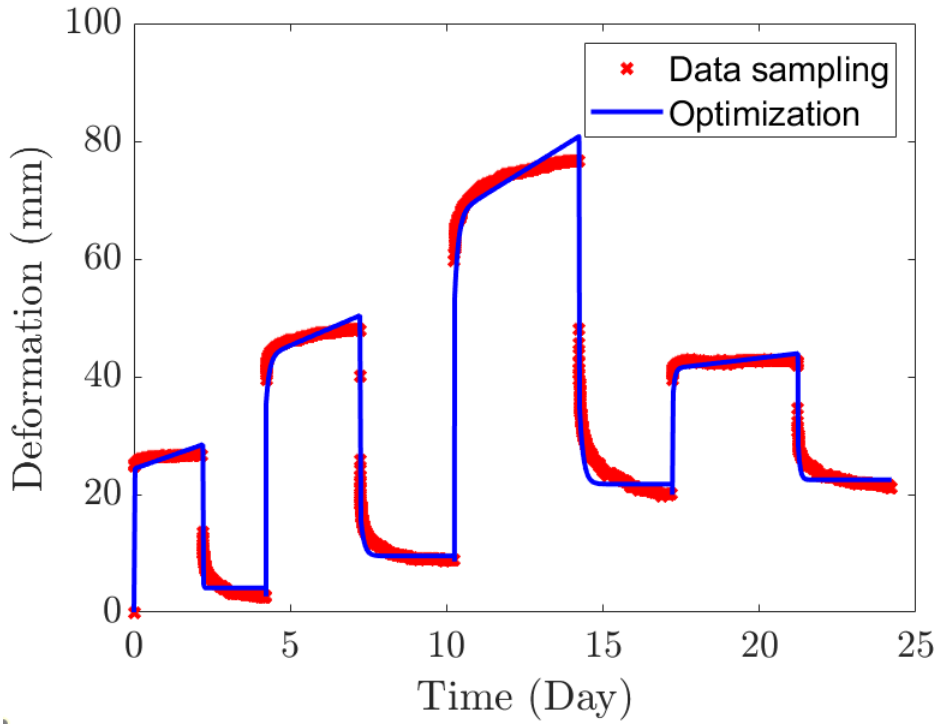

FIGURE 7 – Comparison between estimated and measured cable deformations

lation coefficient will be closer to 1 (-1). The correlation coefficient will be null if two variables are independent.

From Fig. 8, E_2 is highly positively dependent with all the other variables except E_1, with correlation coefficient values of 0.847, 0.930 and 0.800. While E_1 is negatively dependent with all the other variables. Except for E_1, the other variables are all positively dependent with each other, meaning that E_2, η_1 and η_2 decrease when f_i decreases during the optimization, at the same time only E_1 increases in general. Other than E_2, f_i is also strongly positively dependent on η_1, with a correlation coefficient value of 0.866.

4 Conclusion and Future Work

This paper used a cost effective way to perform static load tests on a Vectran® polymer cable to measure cable creep. The tests were conducted for long time periods on a relatively long cable. A standard Burgers material model is proposed to estimate the cable strain, and the parameters in the model used were determined with non-linear least square method to fit the experiment measurements. The correlations between the objective function and the decision variables are analyzed with a scatter matrix. With optimization, the average cable model deformation error was found to be within 0.025% of the initial cable length, and for some loading trials, the average percentages are lower than 0.02%. We can see that the proposed Burgers Model describes the strain shown in the Vectran® cable with good accuracy.

However, it is apparent that the slope of calculated creep varies considerably from the observed creep. This could be due to the fact that polymer cables are braided using complex braiding patterns, and unravelling of these braids causes an unexpected damping effect on the viscoelastic model. It

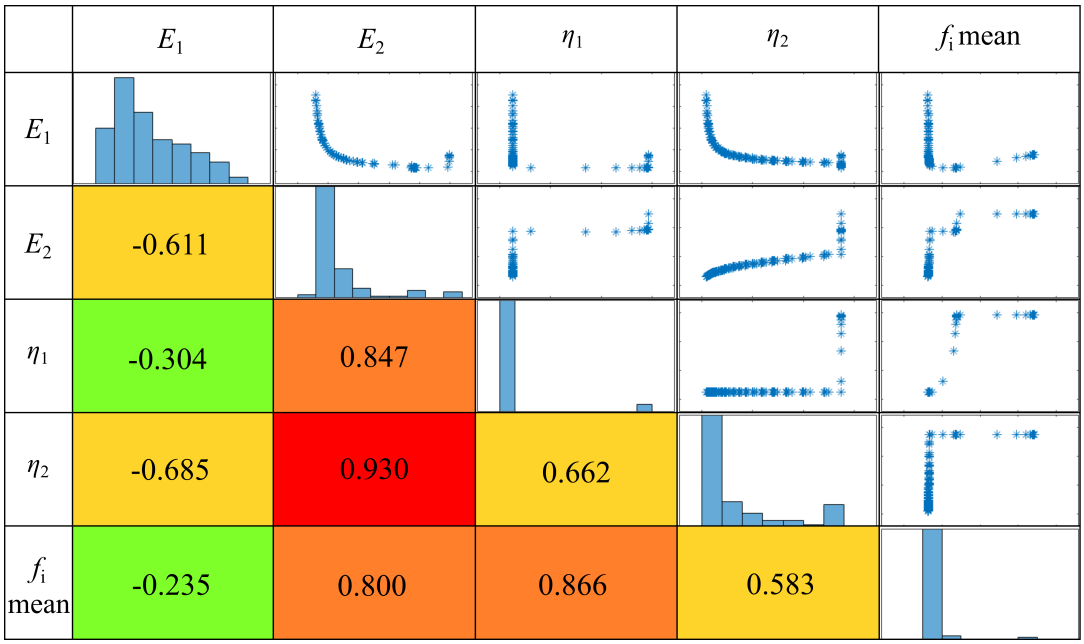

FIGURE 8 – Scatter matrix of the decision variables and the objective function

is suggested in Ref. [14] that a standard (ISO/DIS 19901-7 :2004) exists for conducting creep tests on polymer cables used in offshore structures. This standard suggests five bedding-in cycles of the cable at 50% of its rated load before conducting the creep experiment. Although bedding-in was done before the start of the experiment, our study lacked the facilities to sustain 50% load rating of the VECT017LE cable at 125kg. The importance of this bedding-in cycle is made more apparent by the fact that actual room temperature creep exhibited by Vectran® at 30% loading is less than 0.04% per decade [3]. Since the loads used in our study were well below this threshold, the sort of creep and plastic strain observed contradict existing literature.

In the future, our model will offer a modified Burgers Model to more accurately describe the strain seen in the cable, and particularly for the downward slope observed during cable relaxation. In addition, expansion of experimental setup could allow for bedding-in cycles of the cable in accordance to the latest ISO 19901-7 :2013 standards. Both of these changes could exponentially increase the accuracy of the cable characterization, and aid in even more accurate prediction of CDPR movements.

Acknowledgements

This work was supported by the ANR CRAFT project, grant ANR-18-CE10-0004 (https ://anr.fr/Project-ANR-18-CE10-0004). The research work was motivated by the EquipEx+ TIRREX project, grant ANR-21-ESRE-0015, too. The second author of the paper is grateful for the support of China Scholarship Council (CSC Grant No.202008070051).

Références

[1] L. Gagliardini, S. Caro, M. Gouttefarde, and A. Girin. Discrete reconfiguration planning for cable-driven parallel robots. *Mechanism and Machine Theory*, 100 :313–337, 2016.

[2] S. Kawamura, W. Choe, S. Tanaka, and S.R. Pandian. Development of an ultrahigh speed robot falcon using wire drive system. 1 :215–220 vol.1, 1995.

[3] Hideki Hoshiro, Ryokei Endo, and Forrest Sloan. *Vectran® : Super Fiber from the Thermotropic Crystals of Rigid-Rod Polymer*, pages 171–190. 08 2016.

[4] Sung-Hyun Choi and Kyoung-Su Park. Integrated and nonlinear dynamic model of a polymer cable for low-speed cable-driven parallel robots. *Microsystem Technologies*, 24, 2018.

[5] Jinlong Piao, XueJun Jin, Eunpyo Choi, Jong-Oh Park, Chang-Sei Kim, and Jinwoo Jung. *A Polymer Cable Creep Modeling for a Cable-Driven Parallel Robot in a Heavy Payload Application*, pages 62–72. 07 2018.

[6] John Momoh, Yusuf Shuaib-Babata, and Gabriel ADELEGAN. Modification and performance evaluation of a low cost electro-mechanically operated creep testing machine. *Leonardo Journal of Sciences*, 9, 12 2010.

[7] Peter Davies, Emmanuel Chailleux, Anthony Bunsell, Francois Grosjean, and Michel Francois. Prediction of the long term behavior of synthetic mooring lines. 05 2003.

[8] Maksym Iurzhenko, Yevgen Mamunya, Gisèle Boiteux, Eugene Lebedev, V. Davydenko, Gérard Seytre, and Liubov Matkovska. Creep/Stress Relaxation of Novel Hybrid Organic-Inorganic Polymer Systems Synthesized by Joint Polymerization of Organic and Inorganic Oligomers. *Macromolecular Symposia*, 341 :51–56, July 2014.

[9] Horst Czichos, Tetsuya Saito, and Leslie Smith. *Springer Handbook of Materials Measurement Methods*, volume 153-158. 01 2006.

[10] Kasif Onaran William N Findley, James S Lai. *Creep and relaxation of nonlinear viscoelastic materials, with an introduction to linear viscoelasticity*. North-Holland Publishing Company Amsterdam, New York, NY, 1976.

[11] Kevin Menard and Noah Menard. *Dynamic Mechanical Analysis*. 05 2020.

[12] Arindam Dey and Prabir Basudhar. Applicability of burger model in predicting the response of viscoelastic soil beds. *Geo-Florida–2010 : Advances in Analysis, Modeling and Design, Florida, U.S.A., Geotechnical Special Publication*, GSP :2611–2620, 01 2010.

[13] Dich-Vu Kieu and Shyh-Chour Huang. Dynamic creep phenomenon on polymer cable with non-linear characteristics for cable-driven parallel robots. pages 378–380, 10 2020.

[14] Ghoreishi Reza. *Modelisation analytique et caracterisation experimentale du comportement de cables synthetiques*. Thesis, Ecole centrale de Nantes, 2005.